Electro-mechanical Properties of Functional Fiber-Based Rigid Pavement under Various Loads Applied on a Large-Scale in-Situ Section

Irfan Talib Hameed [1, a*] and Ali Al-Dahawi[2, b]

[1]Karbala Road and Bridge Directorate, Ministry of Construction, Housing, and Municipality, Karbala, Iraq

[2]Civil Engineering Department, University of Technology, Baghdad, Iraq

[a]irfance84@gmail.com and [b]ali.m.aldahawi@uotechnology.edu.iq

*Corresponding author

Abstract. Highways play a critical role in development plans worldwide, as they significantly impact people's daily lives. Monitoring vehicle weights can enhance road lifespan, improve efficiency, and reduce maintenance costs. Self-sensing concrete has emerged as a groundbreaking technology for real-time monitoring structures and infrastructures, including rigid pavement. By incorporating electrically conductive materials (ECMs), this type of concrete can detect and measure load magnitudes. An experimental study investigated the electro-mechanical properties of rigid pavement under various types of loads using chopped carbon fiber (CCF) and macro-end hook steel fiber (SF) on a large-scale in situ section. The applied loads were represented by trucks classified according to Iraqi standards. The study revealed that as the applied loads on the test section increased, the electrical resistivity (ER) decreased accordingly, with the degree of change being directly proportional to the magnitude of the applied stress.

Keywords: Self-sensing; Conductive filler; Multifunctional cementitious composite; Rigid pavement; Electrical resistivity

1. INTRODUCTION

The significance of highways in human life cannot be overstated; they serve as crucial links connecting cities, facilitating transportation, and symbolizing progress and development. These critical lifelines allow us to move efficiently, maintaining our modern way of life and enabling us to thrive in today's world [1,2]. Real-time and precise monitoring of pavement structure stress and deformation is crucial for designing maintenance schemes, quality control during construction, early detection of damage, and preventive measures to maintain the pavement's longevity. This innovative approach offers practical and significant benefits to ensure the optimal performance and safety of the pavement [3]. Structural Health Monitoring (SHM) involves the creation and utilization of methods and techniques for the ongoing supervision and maintenance of a structure's functional value. By implementing SHM, structures can potentially have longer design lives, ensure public safety, and significantly reduce rehabilitation costs. This innovative approach provides continuous monitoring and early detection of potential issues, allowing for prompt remedial action and minimizing the risk of catastrophic failure [4]. Real-time condition assessment and structural health monitoring (SHM) of civil infrastructure can enhance structural safety and increase maintenance service intervals through condition-based maintenance [5]. Self-sensing cement-based structural materials offer the benefit of easily binding with the monitored structure as they possess similar material properties as the structure being monitored [6-9].

There has been a dramatic growth in both vehicle traffic and the need for transportation, putting a significant strain on our nation's highways. Traffic management, maintenance, and operation all benefit from constant eyeballs on the roads and strict limits on how much weight each vehicle may carry [10]. Weigh-in-Motion (WIM) data may be directly utilized to assess degradation, such as that caused by overloaded vehicles [11, 12] or traffic-related tiredness [13]. Underestimating utilization rates of highways can lead to overestimating service life [14] and, therefore, to unanticipated structural breakdown [15]. Overweight trucks may cause more traffic accidents, resulting in crashes in property and life losses [16]. They can potentially disrupt transportation networks, resulting in higher costs for road users, road authorities, and the general public. Han et al. [17] defined self-sensing concrete as the capability to sense the applied stresses, observe the progression of the strain (or deformation) and cracking, and provide warnings about infrastructure deterioration. Traditional traffic detectors have drawbacks such as poor durability, limited sensitivity, low survival rate, and expensive cost. Furthermore, several of these have bad compatibility with pavement surface, which affect negatively the pavement life [18-23].

Electrically conductive materials (ECM) like carbon fibers (CF) were used to reinforce traditional concrete or cementitious composites, resulting in substantial self-sensing concrete [6-9,12,22-26]. These ECMs can increase mechanical properties, boosting their capacity to detect loads, deformations, and cracks without using external embedded or linked sensors. Furthermore, although substantial self-sensing concrete was created from cementitious materials, it offers several benefits, including ease of installation, low cost, easy maintenance, extended surface life, and high compatibility with pavement structure [27-31].

The enormous specific surface area of the conductive fillers impacts the workability of the concrete matrix. To enhance the dispersion of functional fillers, fly ash, silica fume, nano-calcite, and others also aid in the distribution of other components into the concrete matrix. Consequently, they have two dispersion effects, which are helpful to the homogeneity and sensing characteristics of self-sensing concretes [17,32-36]. In addition to improving the mechanical properties of cementitious composites, silica fume or fly ash were utilized to employ conductive elements inside the cementitious composite and minimize the concrete porosity [37,38]. This investigation delves into the practicality of using the piezoresistive characteristics (smart rigid pavement) to effectively observe the movement of vehicles and detect the weight exerted by their axles and wheels. The primary objective is to ensure precise and secure traffic flow monitoring in real-world scenarios.

2. MATERIALS AND MIXTURE PROPERTIES

2.1 Materials

Sulfate-resistant Type 5 Portland cement was used to fabricate the in-situ rigid pavement section [39]. The cement was mixed with Fly Ash (FA) class F, which had a specific gravity of 2.1 and surface area of 296 m^3/kg, following ASTM C-618 standard [40]. To further enhance the conductivity of the mixture, Silica Fume (SFu) was added, which improved the conductive components' dispersion and conformed to the ASTM-C1240 standards [41], with an impressive surface area of 150,000 cm^2/g. Moreover, the 19 mm maximum aggregate size from the al-Nebaey quarry was mixed with fine aggregates from the al-Ekhedher quarry's zone III. The research incorporated two types of conductive fibers: Chopped Carbon Fibers (CCF12) measuring 12mm in length, with a density of 1.7 g/cm^3, a tensile strength of 4200 MPa, and elastic modulus of 240 GPa, as well as Macro End Hook Steel Fibers (SF) with lengths of 30 and 50 mm, a density of 7.8 g/cm^3, the tensile strength of 2850 MPa, and elastic modulus of 200 GPa. The selection of electrode size and characteristics was determined from previous research [6,12], resulting in an electrode made of 70% copper and 30% zinc. The electrodes measure 1mm in width, with a thickness of 1 mm and different lengths depending on their locations within the pavement section. For the study, 19 mm coarse aggregates from the al-Nebaey quarry were paired with fine aggregates from the al-Ekhedher quarry's zone III. The research incorporated two types of conductive fibers: Chopped Carbon Fibers (CCF12) measuring 12 mm in length, with a density of 1.7 g/cm^3, a tensile strength of 4200 MPa, and elastic modulus of 240 GPa, as well as Macro End Hook Steel Fibers (SF) with lengths of 30 and 50 mm, a density of 7.8 g/cm^3, the tensile strength of 2850 MPa, and elastic modulus of 200 GPa as illustrated in Table 1. The electrode size and characteristics selection was determined from previous research [42,43], resulting in an electrode of 70% copper and 30% zinc. The electrode measures 10mm in width and thickness, with a thickness of 1mm.

Table 1: Properties of the conductive materials.

property	Unit	CF	S	
Length	mm	12	30	50
Diameter	µm	7	0.55	0.7
Unit Weight	gm/cm^3	1.7	7.8	7.8
Tensile Strength	Mpa	4150	1650	1800
Tensile Modulus	Gpa	252	200	200

2.2 Mixture Proportions

Banyhussan [44] research established the optimal composition of cementitious materials (including fly ash, cement, and silica fume), aggregate (both coarse and fine), conductive fillers (chopped carbon fiber and steel fiber), water/cement ratio, and high-performance superplasticizer concrete admixture(HPSCA) to create a superior mixture.

2.3 Setup of Electrical Measurement for Mechanical Test

In this study, the self-sensing properties of mixtures were analyzed using the core concept of piezoresistivity, which involves detecting the Fractional change in electrical resistivity (FCER), which can find by using Equation 1 [10] illustrated below:

$$FCER=\frac{\Delta R}{Ro}=\frac{RL-Ro}{Ro} \quad (1)$$

Where: FCER: fractional change in electrical resistance; ΔR: electrical resistance changing (Ω); Ro: initial electrical resistance before the mechanical test started (Ω); R*L*: denotes the electrical resistivity experienced during loading or unloading (Ω). A two-probe DC method was utilized to measure the change in electrical resistance caused by the applied load, and precise digital electrical meters were employed to record the electrical resistance data. This innovative approach enabled the accurate evaluation of the mixtures' self-sensing capabilities, providing valuable insights into their overall performance under different loading conditions.

2.4 Test Section Preparation

The study location was carefully chosen on a heavy-traffic highway in Karbala, approximately 28 kilometers from Al-Ukhadher Fortress. One large test section (rectangular prism) measuring (4×1×0.2) meters is

illustrated in Figure 1. We carefully selected dimensions for the test section with meticulous precision, ensuring that the entire length and contact area of a lone truck's axle would gracefully pass over. Following AASHTOO guidance [45, the truck's maximum width of 2.59 m led to a fair 4-meter width for the section. Figure 2 demonstrates the tire's contact area and guides to allocate 1 meter selectively.

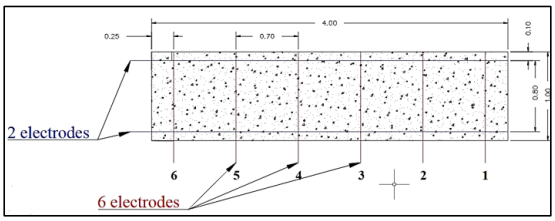

Figure 1: In-situ section and electrode dimensions.

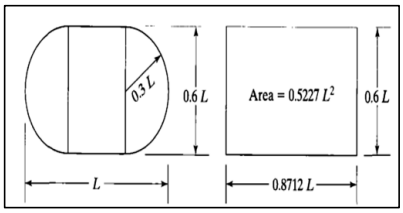

Figure 2: Dimension of tire contact area [46].

Two parallel electrodes were inserted in the section's length, spaced at 0.8m, while six electrodes were added perpendicular to the length, spaced at 0.7m intervals. The electrodes allowed for monitoring of electrical resistivity changes, while a reinforced control cable consisting of 12 single wires in the short direction and another cable with two single wires in the long direction enabled load measurement. The asphalt layer was cut and removed to the proper depth, as depicted in Figure 3. The dimensions were checked, and the electrodes' location was marked, as demonstrated in Figure 4. The concrete was meticulously mixed using a truck mixer. It was then poured into the test section, with great care taken to ensure the correct installation of the electrodes. The resulting test section was crafted to the highest quality through this precise process, providing optimal conditions for accurately analyzing its properties. The area after complete construction and monitoring time is shown in Figure 5.

Figure 3: Checking elevation requirement.

Figure 4: Marking the electrode's location.

Figure 5: In-situ section after opening the road lane.

2.5 Monitoring ER in the Test Section

To measure the changes in electrical resistivity (ER) when loads from passing vehicles are applied. Four trusty electrical resistivity (ER) meters were called into action to achieve this. These meters were cleverly connected to electrode pairs via a control cable, which was meticulously buried in the shoulder of the road, as depicted in Figure 6. The electrical meters were then linked to a computer in a test car parked safely off the highway shoulder, providing the convenience of remote readings monitoring. The computer records all (ER) data and real-time video recordings, as illustrated in Figure 7.

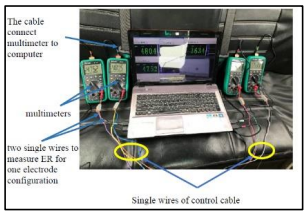

Figure 6: Control cable connection with electrical resistivity meters.

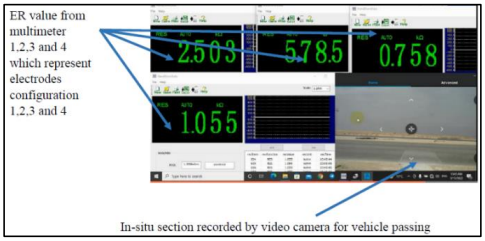

Figure 7: Computer screen displays meters with a live camera.

2.6 Configurations and Dates for the Test Section

It takes several different configurations to settle on the best layouts, which are the more sensitive ones. Time here is so important, especially with the heavy traffic density. The configurations that were used in this study were electrodes (1- 2), (1-6), (2-5), (3-6), and (4-5) for different dates after the construction section, which are (25 to 112 days). Vehicles classification follows the Iraqi standard for the Road and Bridge Department [47], where just three kinds of vehicles were taken (3S1, 3S2, and 3S3).

3. RESULTS AND DISCUSSION

The electrical resistance measured is illustrated in Table 2 below, representing a sample of 593 trucks of the three kinds (3S1, 3S2, and 3S3). Applying equation 1 to the ER for each type constitutes the results by curves, as demonstrated in curves (1 to 5). As shown in Table 4, the electrical resistivity (ER) decreased in all cases when the test section was traversed by trucks. This suggests that the passage of these vehicles increased the conductivity of the concrete in the section. The change in ER, i.e., the Fractional change in Electrical Resistivity (FCER%), was found to be influenced by various factors such as the speed of the truck, the distance between the electrodes measuring ER, and the type of truck used. These findings offer valuable insights into the complex relationship between truck traffic and the electrical properties of concrete.

The distance between the electrodes largely influences the sensitivity of the sensing ability. Interestingly, although the weight of truck 3-S1 is lighter than that of 3-S3, the FCER% of pair 4-5 in 3-S1 is higher than pair 1-6 in 3-S3. This can be attributed to the fact that the distance between pair 4-5 (0.7 m) is smaller than between pair 1-6 (3.5m), as illustrated in Figures 1 and 3 below. These findings shed light on the crucial role of electrode spacing in accurately evaluating the self-sensing properties of mixtures.

Table 2**:** The ER values obtained during the period in which trucks pass over the test section.

Time (sec.)	Pair type													
	1_2			1_6		2_5			3_6			4_5		
	Days after construction													
	77	112		25		25			30		37	77	112	
	Truck type													
	3S1	3S1	3S2	3S2	3S3	3S1	3S2	3S3	3S2	3S3	3S3	3S2	3S1	3S2
	ER (Ω)													
0.5	12130	11910	11860	1197	1187	1367	1185	1242	1355	1921	829	4370	5113	4605
1	12130	11910	11850	1197	1187	1367	1185	1242	1355	1921	829	4367	5113	4606
1.5	12130	11900	11840	1197	1186	1366	1182	1238	1354	1920	828	4366	5113	4605
2	12120	11900	11830	1197	1186	1362	1179	1236	1349	1919	828	4360	5022	4532
2.5	12100	11890	11830	1197	1186	1360	1178	1232	1345	1916	828	4353	5026	4549
3	12090	11890	11830	1196	1186	1359	1177	1231	1345	1907	828	4351	5044	4558
3.5	12090	11890	11840	1196	1186	1359	1176	1233	1344	1905	828	4352	5064	4576
4	12100	11900	11850	1196	1187	1361	1179	1235	1347	1905	827	4353	5074	4596
4.5	12120	11900	11850	1196		1364	1180	1238	1349	1906	827	4361	5094	4604
5	12120	11900	11850	1197		1366	1181	1241	1352	1914	827	4363	5101	4605
5.5	12130	11910	11850	1197		1366	1181	1242	1353	1918	827	4366	5102	
6	12130	11910	11850	1197		1367	1182	1242	1353	1919	828	4367	5103	
6.5	12130	11910	11860	1197		1367	1182		1353	1919	828	4368	5104	
7	12130	11910	11860				1182		1354	1920	829	4369	5107	

Based on the video survey, it was determined that the path of all truck axles passed over pairs 1-2 and 4-5, which provided the most effective sensing compared to other couples. This is because the load area was situated between these pairs, as shown in Figures 8 to 10. By carefully analyzing the survey results, the optimal location for accurate sensing was identified, allowing for enhanced performance and reliability of the sensing system.

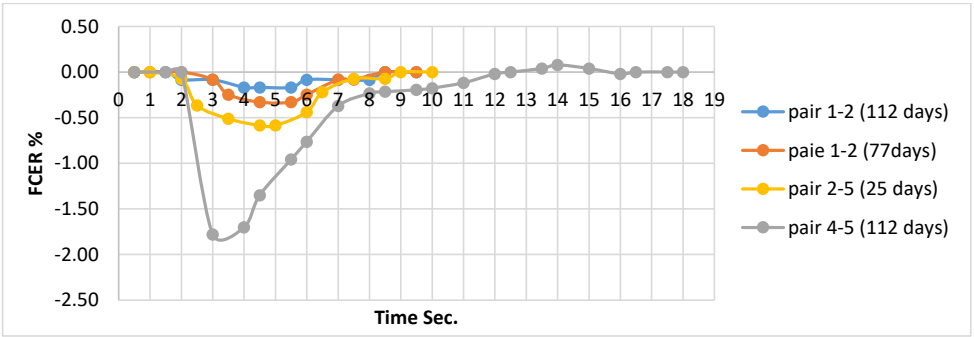

Figure 8: FCER for 3-S1.

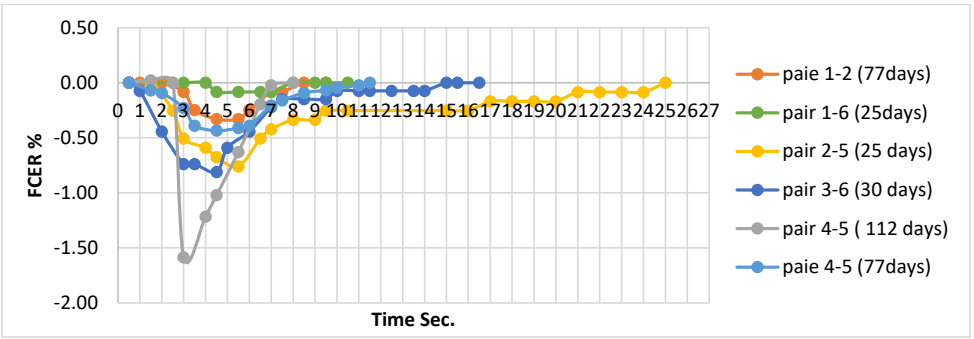

Figure 9: FCER for 3-S2.

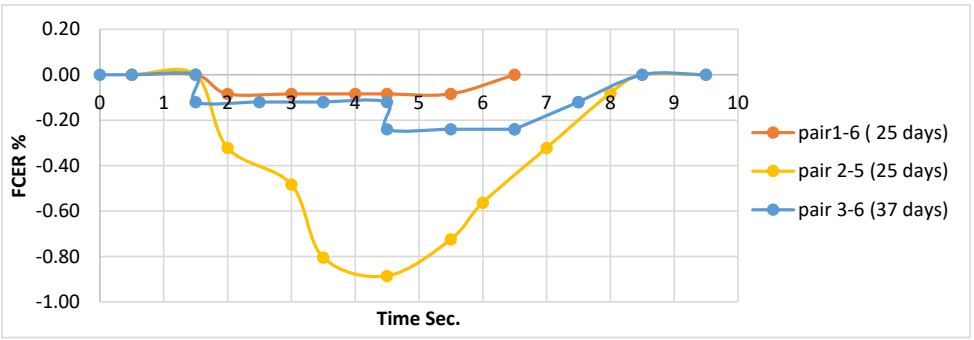

Figure 10: FCER for 3-S3.

The interplay between weight and speed was brought to light during the video survey, revealing that the truck's speed had a detrimental effect on the section's sensing ability. The load could not be sensed in time, rendering the weigh-in-motion (WIM) technology ineffective. This underscores the critical importance of considering the dynamic relationship between weight and speed in the design and implementation.

4. CONCLUSIONS

- Through this study, it has been established that the most effective electrode configurations for the in-situ test section are located under the truck axle (1-2 and 4-5). These configurations offer exceptional sensitivity and recovery time, delivering the best response for electrical resistance (ER) levels.
- The self-sensing concrete pavement can detect and provide crucial traffic data to both small vehicles (passenger cars) and large vehicles (trucks) traveling over the in-situ segment as long as they are moving at approximately 4 km/h. This cutting-edge technology represents a significant advancement in traffic monitoring, allowing for more accurate and efficient data collection, enhancing road safety, and improving traffic flow.
- Measuring an in-situ section's electrical resistance (ER) using a single electrode simultaneously multiple times can negatively impact accuracy and sensitivity, leading to unclear and confusing results. Employing the correct electrode configuration to achieve accurate and reliable data is crucial.
- Capturing accurate electrical resistivity measurements requires careful consideration, as it is crucial to ensure that the polarization of the section is fully completed before recording the results. Taking the necessary time to complete this process is essential to achieving reliable and precise measurements.

REFERENCES

[1] Delatte, N.J. Concrete pavement design, construction, and performance. CRC Press. 2014.
[2] Liang M, Liang P, Fan W, Qian C, Xin X, Shi J, Nan G. Thermo-rheological behavior and compatibility of modified asphalt with various styrene–butadiene structures in SBS copolymers. Materials & design. 2015 Dec 25;88:177-85.
[3] Xue W, Wang L, Wang D, Druta C. Pavement health monitoring system based on an embedded sensing network. Journal of Materials in Civil Engineering. 2014 Oct 1;26(10):04014072.
[4] Sofi A, Regita JJ, Rane B, Lau HH. Structural health monitoring using wireless smart sensor network–An overview. Mechanical Systems and Signal Processing. 2022 Jan 15;163:108113.

[5] Downey A, D'Alessandro A, Baquera M, García-Macías E, Rolfes D, Ubertini F, Laflamme S, Castro-Triguero R. Damage detection, localization and quantification in conductive smart concrete structures using a resistor mesh model. Engineering Structures. 2017 Oct 1;148:924-35.
[6] Al-Dahawi A, Yıldırım G, Öztürk O, Şahmaran M. Assessment of self-sensing capability of Engineered Cementitious Composites within the elastic and plastic ranges of cyclic flexural loading. Construction and Building Materials. 2017 Aug 1;145:1-0.
[7] Al-Dahawi AM. Effect of curing age on the self-sensing behavior of carbon-based engineered cementitious composites (ECC) under monotonic flexural loading scenario. InMATEC Web of Conferences 2018 (Vol. 162, p. 01034). EDP Sciences.
[8] Yıldırım G, Sarwary MH, Al-Dahawi A, Öztürk O, Anıl Ö, Şahmaran M. Piezoresistive behavior of CF-and CNT-based reinforced concrete beams subjected to static flexural loading: Shear failure investigation. Construction and Building Materials. 2018 Apr 20;168:266-79.
[9] Sarwary MH, Yıldırım G, Al-Dahawi A, Anıl Ö, Khiavi KA, Toklu K, Şahmaran M. Self-sensing of flexural damage in large-scale steel-reinforced mortar beams. ACI Materials Journal. 2019 Jul 1;116(4):209-21.
[10] Al-Dahawi, A. Multifunctional Cementitious Composites for Damage-Resistance Highway Structures, in Civil Engineering. Univesity of Gaziantep: Gaziantep, Turkey. 2016.
[11] Al-Qadi I, Wang H, Ouyang Y, Grimmelsman K, Purdy JE. LTBP Program's Literature Review on Weigh-in-Motion Systems. 2016.
[12] Ghadhban, D., H.H. Joni, and A.M. Al-Dahawi. Carbon Fiber-Based Cementitious Composites for Traffic Detection and Weighing In Motion. Engineering and Technology Journal. 2021; 39(8): 1250-1256.
[13] Sujon, M. and F. Dai. Application of weigh-in-motion technologies for pavement and bridge response monitoring: State-of-the-art review. Automation in Construction. 2021.
[14] Andrle, S., B. McCall, and D. Kroeger. Application of weigh-in-motion (WIM) technologies in overweight vehicle enforcement. In 3rd International Conference on Weigh-in-Motion (ICWIM3). Citeseer. 2002.
[15] Lehman, Maria. The American Society of Civil Engineers' report card on America's infrastructure. In: Women in Infrastructure. Cham: Springer International Publishing. 2022.
[16] ZHANG, Yuhuan; LU, Huapu; QU, Wencong. Geographical detection of traffic accidents spatial stratified heterogeneity and influence factors. International journal of environmental research and public health. 2020; 17(2): 572.
[17] Han B, Wang Y, Dong S, Zhang L, Ding S, Yu X, Ou J. Smart concretes and structures: A review. Journal of intelligent material systems and structures. 2015 Jul;26(11):1303-45.
[18] Li GY, Wang PM, Zhao X. Pressure-sensitive properties and microstructure of carbon nanotube reinforced cement composites. Cement and Concrete Composites. 2007 May 1;29(5):377-82.
[19] Gupta S, Lin YA, Lee HJ, Buscheck J, Wu R, Lynch JP, Garg N, Loh KJ. In situ crack mapping of large-scale self-sensing concrete pavements using electrical resistance tomography. Cement and Concrete Composites. 2021 Sep 1;122:104154.
[20] Wang H, Shi F, Shen J, Zhang A, Zhang L, Huang H, Liu J, Jin K, Feng L, Tang Z. Research on the self-sensing and mechanical properties of aligned stainless steel fiber-reinforced reactive powder concrete. Cement and Concrete Composites. 2021 May 1;119:104001.
[21] Armoosh SR, Oltulu M, Alameri I, Mohammed HM, Karacali T. The combined effect of carbon fiber and carbon nanotubes on the electrical and self-heating properties of cement composites. Journal of Intelligent Material Systems and Structures. 2022 Nov;33(18):2271-84.
[22] Al-Dahawi A, Öztürk O, Emami F, Yıldırım G, Şahmaran M. Effect of mixing methods on the electrical properties of cementitious composites incorporating different carbon-based materials. Construction and Building Materials. 2016 Feb 1;104:160-8.
[23] Celik DN, Yıldırım G, Al-Dahawi A, Ulugöl H, Han B, Şahmaran M. Self-monitoring of flexural fatigue damage in large-scale steel-reinforced cementitious composite beams. Cement and Concrete Composites. 2021 Oct 1;123:104183.
[24] Dong W, Li W, Zhu X, Sheng D, Shah SP. Multifunctional cementitious composites with integrated self-sensing and hydrophobic capacities toward smart structural health monitoring. Cement and Concrete Composites. 2021 Apr 1;118:103962.
[25] Al-Dahawi A, Sarwary MH, Öztürk O, Yıldırım G, Akın A, Şahmaran M, Lachemi M. Electrical percolation threshold of cementitious composites possessing self-sensing functionality incorporating different carbon-based materials. Smart Materials and Structures. 2016 Sep 16;25(10):105005.
[26] Yıldırım G, Öztürk O, Al-Dahawi A, Ulu AA, Şahmaran M. Self-sensing capability of Engineered Cementitious Composites: Effects of aging and loading conditions. Construction and Building Materials. 2020 Jan 20;231:117132.
[27] Shi, Z.-Q. and D. Chung. Carbon fiber-reinforced concrete for traffic monitoring and weighing in motion. Cement and Concrete Research. 1999; 29(3): 435-439.
[28] Han, B. and J. Ou. Embedded piezoresistive cement-based stress/strain sensor. Sensors and Actuators A: Physical. 2007; 138(2): 294-298.

[29] Chung, D.D.L. Self-sensing concrete: from resistance-based sensing to capacitance-based sensing. International Journal of Smart and Nano Materials. 2021; 12(1): 1-19.
[30] Xu J, Yin T, Wang Y, Liu L. Anisotropic electrical and piezoresistive sensing properties of cement-based sensors with aligned carbon fibers. Cement and Concrete Composites. 2021 Feb 1;116:103873.
[31] Li W, Dong W, Guo Y, Wang K, Shah SP. Advances in multifunctional cementitious composites with conductive carbon nanomaterials for smart infrastructure. Cement and Concrete Composites. 2022 Apr 1;128:104454.
[32] Nuaklong P, Wongsa A, Boonserm K, Ngohpok C, Jongvivatsakul P, Sata V, Sukontasukkul P, Chindaprasirt P. Enhancement of mechanical properties of fly ash geopolymer containing fine recycled concrete aggregate with micro carbon fiber. Journal of Building Engineering. 2021 Sep 1;41:102403.
[33] Karkush MO, Abdulkareem MS. Deep remediation and improvement of soil contaminated with residues oil using lime piles. International Journal of Environmental Science and Technology. 2019 Nov;16:7197-206.
[34] Karkush MO, Yassin SA. Using sustainable material in improvement the geotechnical properties of soft clayey soil. Journal of Engineering Science and Technology. 2020 Aug;15(4):2208-22.
[35] Karkush MO, Ali HA, Ahmed BA. Improvement of unconfined compressive strength of soft clay by grouting gel and silica fume. InProceedings of China-Europe Conference on Geotechnical Engineering: Volume 1 2018 (pp. 546-550). Springer International Publishing.
[36] Karkush MO, Almurshedi AD, Karim HH. Investigation of the Impacts of Nanomaterials on the Micromechanical Properties of Gypseous Soils. Arabian Journal for Science and Engineering. 2023 Jan;48(1):665-75.
[37] CHUNG, Deborah DL. Composite materials: science and applications. Springer Science & Business Media. 2010.
[38] YI, Fang; KAIQIN, Chen; MAN, Zhu. Preparation and mechanical-electrical performance of carbon fibre sensing concrete. Ceramics–Silikáty. 2022; 66(1): 28-35.
[39] ASTM-C150. Standard specification for Portland cement, in Annual book of ASTM standards. 2007.
[40] ASTM-C618. Standard specification for coal fly ash and raw or calcined natural pozzolan for use in concrete. Annual book of ASTM standards. 2005.
[41] ASTM-C1240-20. Standard Specification for Silica Fume Used in Cementitious Mixtures. ASTM: USA. 2020.
[42] Al-Dahawi, A. Multifunctional Cementitious Composites For Damage-Resistant Highway Structures. in Civil Engineering, Univesity of Gaziantep: Gaziantep, Turkey. 2016.
[43] Mohammed, A.K., Development of Optimal Deflection Hardening and Self-Sensing Cementitious Composites for Concrete Pavement. 2020.
[44] Banyhussan, Q.S. Development of Optimal Strain Hardening Cementitious Composites Mixture for Highway Bridge Decks to Address Shrinkage Cracking. 2017.
[45] AASHTO, Transportation Officials, DC, Policy on geometric design of highways and streets. 2017; 1(990): 158.
[46] Huang, Y.H. Pavement analysis and design. Pearson Prentice Hall Upper Saddle River, NJ. 2004.
[47] SCRB. Highway Design Manual in The Vehicle. Ministry of Housing, Construction and Municipality, Department of Planning and Studies: Iraq. 2005.